A SECOND-ORDER CLOSURE MODEL FOR FLOW THROUGH VEGETATION

J. D. WILSON

University of Alberta, Edmonton, Alberta, Canada

(Received in final form 3 August, 1987)

Abstract. By splitting the turbulent kinetic energy into two wavebands and adopting as the turbulence timescale the ratio k/ε of the kinetic energy in the low-frequency band to its turnover-rate, the second-order closure scheme of Launder *et al.* (1975) has been adapted for flow through vegetation. Predictions of the model compare satisfactorily with observations of the mean windspeed and (somewhat less satisfactorily) with the turbulent velocity variances in two very different canopies.

1. Introduction

There are several reasons for wishing to predict the nature of turbulent flow through vegetation on the basis of a few simple inputs (e.g., a physical description of the crop or forest, and values of wind-speed, temperature, humidity, and net radiation at some reference height above the canopy). As examples, one may cite concern with understanding the process by which a forest acts as a sink for harmful pollutants, and the ongoing efforts to understand (and perhaps thereby beneficially manipulate) crop interaction with the environment. Several disciplines (hydrology, agricultural and forestry science, meteorology, soil science) share an interest in being able to predict canopy evapotranspiration.

Prediction of canopy flow is in principle pre-requisite to or co-requisite with prediction of the simpler (but itself complex) problem of scalar diffusion (heat, water vapor, carbon dioxide, etc.) within a canopy. On the other hand, Raupach (1987) has shown that the Lagrangian approach to scalar transport yields qualitatively-reasonable results for diffusion from arbitrary but complex source distributions even with a very crude description of the canopy flow (homogeneous turbulence, no mean wind shear). Coupled with the fact (discussed in Section 6) that the transfer resistances moderating the source strength in natural canopies are usually relatively insensitive to windspeed, Raupach's finding supports the argument (J. M. Norman, personal communication) that in most circumstances (except perhaps very light winds) the flow need not be known in great detail in order to predict heat, vapor, and CO_2 diffusion with sufficient accuracy to predict crop growth rate (the latter, of course, depending on other factors).

Attempts to predict canopy flow are at present restricted to the Eulerian formulation. The purely conceptual case of two-dimensional inviscid flow allows a Lagrangian treatment (because vorticity is then conserved). Progress is being made in the simulation of real high-Reynolds-number flows by the (Lagrangian) 'random vortex method' (a review is given by Leonard, 1985), but for the time being, restricted computer power limits application to flows which are nearly everywhere irrotational so that relatively

Boundary-Layer Meteorology **42** (1988) 371–392.

small numbers of vortex elements need to be tracked. In contrast, mass transport may readily be predicted using Lagrangian 'random walk' methods because the governing equation is a simple convection-diffusion equation – whereas the instantaneous vorticity and momentum transport equations are complicated, respectively, by the vortex-stretching/tilting terms and pressure-gradient terms. A readily observable consequence of this distinction between mass and momentum transport is that momentum sources/sinks can cause upstream influence under conditions in which a co-located scalar source would simply produce a downstream advective-diffusive plume.

Given that we are currently restricted to the Eulerian approach and given the impossibility of implementing simulations on a grid sufficiently fine to resolve the smallest eddies and variations in canopy structure, some form of averaging of the governing equations is necessary. In the past ten years, there have been fundamental examinations concerned with proper spatial averaging of canopy flow statistics and development of the correspondingly-averaged budget equations governing the flow (Wilson and Shaw, 1977; Raupach and Shaw, 1982; Finnigan, 1985). There have also been several important canopy flow experiments.

The wind tunnel canopy flow experiment of Raupach *et al.* (1986) included an investigation of the importance of complex terms such as dispersive fluxes (fluxes due to correlated spatial variation of the time-average statistics) which appear in the spatially-averaged budget equations. (It had been recognized for some time that dispersive fluxes were potentially of importance in the flow above very rough surfaces; see for example, Mulhearn, 1978; Mulhearn and Finnigan, 1978.)

The conditional sampling analyses by Finnigan (1979), Shaw *et al.* (1983), and Raupach *et al.* (1986) have revealed the highly intermittent nature of canopy turbulence and the overwhelming importance of occasional penetrations of the canopy by gusts. It has been found that deep within a variety of canopies, local production rates of property variance and flux are negligible in comparison with the rate of import from higher levels, which is represented in the budget equations by the corresponding turbulent transport terms. To quote Finnigan (1985), 'the role of large eddies is described by the transport terms in the second-order equations. In the language of spectral analysis, we would say that the transport term is weighted to low wave numbers'.

An important aspect of this new physical insight into the nature of canopy flow is that it clarifies the observation that first-order closure (K-theory) does not provide a physically satisfactory parameterisation of the turbulent fluxes, which may in fact be directed against the corresponding mean gradient. If one wishes to derive a more rigorous version of K-theory from the second-order equations, it is necessary, among other things, to drop the very turbulent transport terms which have now been shown to be significant. In consequence, most recent attempts to simulate canopy flow numerically have employed higher-order closure. (As will be discussed in Section 2, concern remains that most higher-order models in effect employ K-theory at a higher level.) An exception to this is the work of Li *et al.* (1985) who presented a first-order closure model in which an additional (and empirical) term was added to the streamwise momentum equation to enhance the predicted penetration of the momentum flux. Good agreement

between measured and predicted wind-profiles for a corn canopy and a pine forest was demonstrated, but there were six constants available to be assigned (specifically the drag coefficient, their α, β, c_2, and the two constants appearing in their Equation (7a)).

Wilson and Shaw (1977) demonstrated that reasonable agreement with observations may be obtained using second-order closure. (Higher-order closure schemes themselves yield numerous assignable constants; however, it is normal practise for these to be optimised with reference to some basic flow, perhaps homogeneous isotropic turbulence, and left unchanged in the application to more complex flow.) Meyers and Paw U (1986) adopted third-order closure in order to improve the simulation of the triple-velocity correlation terms (i.e., the transport terms) appearing in the stress budget equations which, to reiterate, are now known to be of great importance. Meyers and Paw U were able to predict wind profiles satisfactorily within a number of very different canopies (the drag coefficient being chosen for each canopy to give optimum agreement).

This paper presents a second-order closure model for neutrally-stratified flow through a horizontally-uniform canopy which differs in several respects from earlier second-order models. The basic closure scheme used here was developed by Launder *et al.* (1975, hereafter LRR), and Hanjalic and Launder (1972). It has proven successful in a wide range of flows without modification of empirical constants (which were initially optimised by LRR). It was hoped that this closure scheme might be applicable without modification to canopy flow, but this proved not to be the case.

The author wished to avoid the necessity, common to all prior higher-order closure canopy-flow models, of arbitrarily specifying a 'time-scale' for the turbulence. The LRR closure scheme satisfies this aim, in that the required timescale is formed as k/ε, where k is the turbulent kinetic energy (TKE) and ε the rate of dissipation of the TKE.

The general line of development used to adapt the LRR scheme to canopy flow was to follow the suggestion of Hanjalic *et al.* (1980) that the TKE be split into two or more (in the present case 2) frequency bands. This is a particularly useful idea for canopy flow because of the complex energy transformations caused by viscous and form drag on the vegetation. Within a canopy, these drag forces not only bring about 'wake production', the conversion of mean flow kinetic energy (MKE) to turbulent kinetic energy, but also extract energy from the turbulent eddies and convert this to turbulent energy at very small (element wake) scales, thereby acting in addition to the normal energy cascade process.

The experimental evidence (Raupach and Shaw, 1982; Raupach and Thom, 1981) is that although the rate of wake production of TKE is comparable to the shear production rate, turbulence on the scale of the element wakes is not a large proportion of the total variance, presumably being subject to very rapid dissipation due to its small scale*. We may, therefore, anticipate that it would be advantageous to separate the TKE into at least two frequency bands and, guided by intuition and observation, estimate the transfers into and out of each band. A diagnostic analysis of experimental canopy

* A similar situation is believed to exist in the near wake of porous windbreaks, where in spite of strong MKE → TKE conversion at the fence, leeward TKE levels are strongly reduced relative to the approaching flow (Wilson, 1985).

turbulence data (from a corn canopy and from a wind tunnel experiment) was carried out by Shaw and Seginer (1985). These authors discussed the kinetic energy balance by splitting the TKE into two frequency bands, which they denoted 'turbulent shear kinetic energy' (SKE, low-frequency band) and 'wake kinetic energy' (WKE, high-frequency band). Symbolic budget equations for each band were written, based on the overall constraint of conservation of energy, and the term corresponding to conversion of SKE to WKE was evaluated directly. In the case of the corn canopy, wake conversion of SKE to WKE was found to balance shear production and turbulent transport (so that the normal energy cascade by vortex stretching was bypassed) and in the artificial canopy, this term was also the most important sink for large scale TKE.

Ideally, a turbulence model would correctly simulate the entire turbulent kinetic energy spectrum and its response to flow distortion and flow/solid interactions. For example, McAneney and Judd (1987) discuss the damaging oscillation of kiwi fruit in response to excitation by gusts at or near the natural frequency of the fruit and argue that different trellice and shelter strategies may augment or diminish the spectral power at these damaging frequencies. Adoption of a two-band model (able to describe the spectrum in terms of a pair of time-scales) is a (very small) step towards prediction of the full spectrum.

The present second-order model uses an emperical formulation of the rate of conversion from SKE to WKE. It differs further from the original LRR closure scheme in the parameterisation of the triple-velocity correlations.

The following sections will give the governing equations, a description of the numerical solution procedure, and a comparison of numerical solutions with observations for both a corn canopy and an artificial wind-tunnel canopy.

2. Governing Equations

Wilson and Shaw (1977) showed that if horizontal averaging is performed with due attention to the fact that the equations of motion are valid only within airspace, extra terms arise which may be formally identified with the canopy-airflow interaction. Raupach and Shaw (1982) and Finnigan (1985) have, respectively, presented time/horizontal-plane and time/volume-averaging schemes, and there is no doubt as to the valuable role of these methods as a means to ensure that self-consistent parameterisations of canopy flow are employed.

Ideally, one would derive from the Navier–Stokes equations the governing equations for the variance (or covariance, etc.) within any frequency band, i.e., governing equations for SKE, WKE, and for any other quantity whose level it is deemed necessary to describe using frequency bands. Proper averaging of these equations should then ensure consistency, so that a parameterisation of source terms in the mean momentum equation would methodically imply corresponding terms in other equations. However, one cannot adopt band-average budget equations on an intuitive basis and expect that the rigorously-derived 'whole spectrum' equation will give the correct rules for consistency of parameterisation. Therefore, the author has not attempted to derive

plant/airflow interaction terms in the budget equations for high-order statistics; just as it proves counter-productive to account for MKE → TKE conversion except if this energy is placed in a high-frequency band, it may be counter-productive to include extra terms in, say, the 'whole spectrum' budget equation for $\overline{w' u' w'}$.

Conservation of streamwise (x) momentum is expressed by

$$\frac{\partial \overline{u' w'}}{\partial z} = -c_d a \bar{u} |\bar{u}| \tag{1}$$

where $a(z)$ is the leaf area density [m^2/m^3]. The momentum sink term on the right-hand side of Equation (1) is a conventional parameterization of the plant-airflow interaction.

The dual band TKE balance used here is a similar but simplified version of that outlined by Shaw and Seginer (1985). For convenience, the low-frequency-band turbulent kinetic energy, SKE, will be denoted by k, the rate of loss of SKE to WKE by ε_{fd}, and the rate of viscous dissipation of SKE by ε_{cc}. Then $\varepsilon = \varepsilon_{fd} + \varepsilon_{cc}$ is the total rate of loss of SKE, and the ratio k/ε will be used as the turbulence time-scale which appears in the closure scheme.

The budget equations for the tangential stress and the low-frequency band (SKE band) normal stresses may be written symbolically as

$$\frac{\partial \overline{u_i' u_j'}}{\partial t} = 0 = P_{ij} + R_{ij} + T_{ij} - \varepsilon_{ij}, \tag{2}$$

where the terms are, respectively,

(a) PRODUCTION

$$P_{xx} = -2\overline{u' w'} \frac{\partial \bar{u}}{\partial z}, \qquad P_{yy} = P_{zz} = 0, \qquad P_{xz} = -\overline{w'^2} \frac{\partial \bar{u}}{\partial z}.$$

(b) REDISTRIBUTION (PRESSURE STRAIN)

$$R_{ij} = \overline{\frac{p'}{\rho_0}\left(\frac{\partial u_i'}{\partial x_j} + \frac{\partial u_j'}{\partial x_i}\right)}.$$

These terms have been parameterised as

$$R_{ij} = R_{ij,1} + R_{ij,2} + R'_{ij,1}$$

where

$$R_{ij,1} = -c_1 \varepsilon/k(\overline{u_i' u_j'} - \tfrac{2}{3}\delta_{ij} k),$$

$$R_{ij,2} = -c_2(P_{ij} - \tfrac{2}{3}P\delta_{ij}),$$

$$R'_{ij,1} = c'_1 \varepsilon/k(\overline{u_k' u_m'} n_k n_m \delta_{ij} - \tfrac{3}{2}\overline{u_k' u_i'} n_k n_j - \tfrac{3}{2}\overline{u_k' u_j'} n_k n_i) f\left(\frac{l}{z}\right).$$

Here $P = \overline{u'w'}(\partial\bar{u}/\partial z)$ is the SKE production rate. The combination $R_{ij,1} + R_{ij,2}$ is the simplified pressure-strain model of LRR. The added term $R'_{ij,1}$ is a wall-proximity correction to the pressure-strain and is necessary to yield the relatively large ratio of streamwise to wall-normal velocity variance (in our case $\overline{u'^2}/\overline{w'^2}$) found in wall flows compared to the corresponding variance ratio in free turbulent flows. The n_k appearing in $R'_{ij,1}$ are components of the unit vector normal to the surface ($n_k = \delta_{k3}$). The form used here for $R'_{ij,1}$ was suggested by Shir (1973) and used by Gibson and Launder (1978). The wall-proximity function has been evaluated as

$$f(l/z) = C_{f1z}(k^{3/2}/\varepsilon)/z\,,$$

with $C_{f1z} = 1.0/(k_v k^{3/2})$, where k_v is von Kármán's constant ($k_v = 0.4$ herein). With this choice for C_{f1z}, the function $f(l/z)$ has the value unity in the case where the flow is in local equilibrium.

Note that R_{ii} and each of its constituents vanish – the redistribution terms disappear in the SKE budget. These terms represent interchange of SKE from component to component and in the absence of a wall, act to return the turbulence towards isotropy.

(c) Transport

Neglecting pressure transport, one has $T_{ij} = -(\partial/\partial z)\overline{w' u'_i u'_j}$.

In order to parameterise $\overline{u'_i u'_j u'_k}$, Hanjalic and Launder (1972) simplified the corresponding budget equation by neglecting shear production, adopting the quasi-Gaussian hypothesis for the quadruple velocity correlation, and replacing the terms involving pressure with a simple return-towards-isotropy term:

$$-\overline{u'_i u'_j u'_k} = c_s \frac{k}{\varepsilon}\left[\overline{u'_i u'_l}\,\frac{\partial\overline{u'_j u'_k}}{\partial x_l} + \overline{u'_j u'_l}\,\frac{\partial\overline{u'_i u'_k}}{\partial x_l} + \overline{u'_k u'_l}\,\frac{\partial\overline{u'_i u'_j}}{\partial x_l}\right].$$

In order to increase the predicted velocity variance within the canopy, the value of c_s has herein been modified according to

$$c_s = c_{s0}(1 + \mathrm{LAI}\,\sin(\pi z/H))\,, \quad z \leqq H\,;$$

where $c_{s0} = 0.11$ (the value recommended by LRR) and LAI is the leaf area index.

A serious theoretical objection to this type of parameterisation of the transport terms is that in effect, a gradient-diffusion formulation is involved. For example, the gradient $\partial\overline{w'^3}/\partial z$ appears in the budget equation for $\overline{w'^2}$, and under the present scheme $\overline{w'^3}$ is parameterised as

$$\overline{w'^3} = -K^{\mathrm{eff}}\frac{\partial\overline{w'^2}}{\partial z}\,,$$

where the 'effective diffusivity' is $K^{\text{eff}} = 3c_s(k/\varepsilon)\overline{w'^2}$. For comparison, the first-order mass diffusion parameterisation is

$$\overline{w'c'} = -K\frac{\partial \bar{c}}{\partial z}$$

for the vertical flux of a scalar whose instantaneous concentration is $c = \bar{c} + c'$. It is a well-known consequence of Taylor's (1921) exact theory of diffusion in homogeneous turbulence that close to a source (i.e., within a small number of times-scales or length scales from the source) the mass diffusivity K depends upon time since release (or distance from the source); the far-field value $\sigma^2 \tau_L$ (a property of the turbulence, since σ is the standard-deviation of the velocity fluctuation and τ_L is a Langrangian time-scale) is merely the upper bound. Deardorff (1978) has shown that if one is to describe diffusion from sources in homogeneous turbulence using higher-order closure of the Eulerian conservation equations, the effective diffusion coefficient which appears at higher-order retains a dependence on time since release (or distance from the source). Deardorff concludes that the higher-order closure methods are 'inherently unable to solve the diffusion problem accurately in the general case of pollutants being released at various points at different times' and that 'any assertion that the closure constants are universal has little relevance in practise'.

There is no reason to believe that these theoretical prohibitions on the use of a gradient-diffusion model at higher order are not equally applicable to the case (of predominant concern here) of momentum transport. An alleviating factor for many applications of higher-order flow models is that usually the momentum sources and sinks will be located at walls (where the turbulence length and time-scales will be small) rather than being distributed within the flow domain. This is clearly not the case for canopy flow, the vegetation in effect being a distributed momentum sink.

(d) Dissipation

It has been assumed that ε_{ij} vanishes unless $i = j$. The values ε_{xx}, ε_{yy}, ε_{zz} are the rates at which low-frequency-band (SKE-band) variance is transferred to WKE or converted to internal energy. It is assumed that the instantaneous drag vector has magnitude $c_d a(u^2 + v^2 + w^2)$, lies opposed to the instantaneous wind vector, and has components

$$FD_x = c_d a u\sqrt{u^2 + v^2 + w^2},$$

$$FD_y = c_d a v\sqrt{u^2 + v^2 + w^2},$$

$$FD_z = c_d a w\sqrt{u^2 + v^2 + w^2}.$$

Assuming $u \gg |v|, |w|$ (which is not a very safe assumption, especially deep in the canopy), one may write

$$FD_x \cong c_d a u^2, \qquad FD_y \cong c_d a u v, \qquad FD_z \cong c_d u w.$$

By splitting variables into mean and fluctuation, and averaging in the normal way, one obtains, here showing only leading terms in $c_d a$

$$\frac{\partial \overline{u'^2}}{\partial t} = -4c_d a\bar{u}\,\overline{u'^2} + \cdots,$$

$$\frac{\partial \overline{v'^2}}{\partial t} = -2c_d a\bar{u}\,\overline{v'^2} + \cdots,$$

$$\frac{\partial \overline{w'^2}}{\partial t} = -2c_d a\bar{u}\,\overline{w'^2} + \cdots.$$

The rate of loss of SKE to WKE is, therefore, approximated as

$$\varepsilon_{fd} = \tfrac{1}{2}c_d a\bar{u}(4\overline{u'^2} + 2\overline{v'^2} + 2\overline{w'^2}); \tag{3}$$

and $\varepsilon = \varepsilon_{fd} + \varepsilon_{cc}$. Viscous dissipation has been parameterised as

$$\varepsilon_{cc} = \frac{(c_3 k)^{3/2}}{k_v z},$$

which is the correct form in the absence of a canopy. Then

$$\varepsilon_{xx} = 4c_d a\bar{u}\,\overline{u'^2} + \tfrac{2}{3}\varepsilon_{cc}, \quad \varepsilon_{yy} = 2c_d a\bar{u}\,\overline{v'^2} + \tfrac{2}{3}\varepsilon_{cc}, \quad \varepsilon_z = 2c_d a\bar{u}\,\overline{w'^2} + \tfrac{2}{3}\varepsilon_{cc}.$$

The energy transformation pathways incorporated in the model are shown in Figure 1.

Shaw and Seginer (1985) estimated the rate of conversion of SKE to WKE to be

$$c_d a(\overline{V^3} - \bar{u}\,\overline{uV}),$$

where V is the instantaneous wind speed (their literal result has here been doubled in accordance with the author's habit of not including a factor of $\frac{1}{2}$ in Equation (1)). The expression used here, Equation (3), may be shown to be the leading term following from Shaw and Seginer's expression on the dubious assumption that $|v/u|, |w/u| < 1$.

The budget equation for WKE is assumed to be

$$\begin{aligned} 0 = {} & \tfrac{1}{2}c_d a\bar{u}(4\overline{u'^2} + 2\overline{v'^2} + 2\overline{w'^2}), && \text{SKE} \rightarrow \text{WKE} \\ & + c_d a\bar{u}^3, && \text{MKE} \rightarrow \text{TKE} \\ & + T - \varepsilon_{\text{WKE}}. \end{aligned} \tag{4}$$

Transport is parameterised as $T = (\partial/\partial z)\,[c_s k/\varepsilon \overline{w'^2}\,(\partial \text{WKE}/\partial z)]$ and dissipation as $\varepsilon_{\text{WKE}} \propto (\text{WKE})^{3/2}/l$, where l = minimum $(c_4 d, k_v z)$ with d being an estimated length scale for the wake turbulence. In simulations carried out to date, the calculated level of WKE has had no feedback effect upon the levels of SKE, mean velocity, or Reynolds stress, so that there is in fact no necessity to include Equation (4).

The governing equations have been cast in dimensionless form using scales H and u_{*H}. The actual velocity at any height which corresponds to a specific reference (above

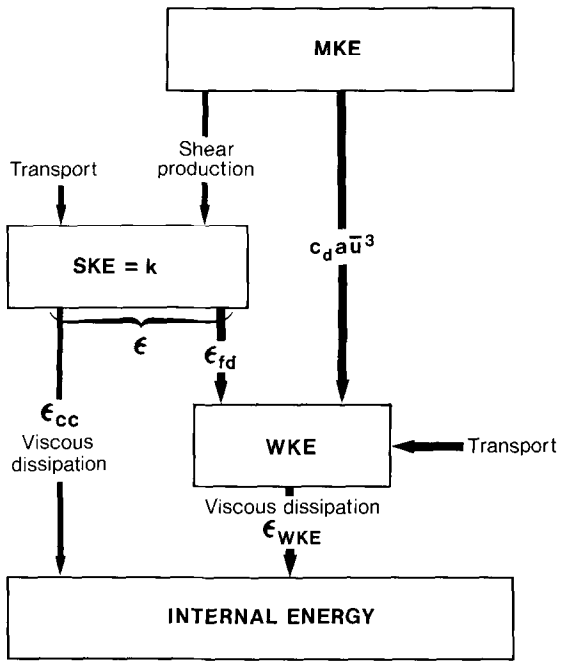

Fig. 1. Schematic of the kinetic energy transformation pathways included in the model. The heavy arrows denote transformations due to the vegetation inbedded in the flow. Symbols are defined in Section 2.

canopy) velocity $\bar{u}_{\text{ref}}$ may easily be obtained from the dimensionless predictions because the value of $\bar{u}_{\text{ref}}/u_{*H}$ will itself be predicted by the model.

On the assumption of a neutral surface layer in local equilibrium (advection and transport of the TKE negligible, TKE production rate = dissipation rate; height-independent $\overline{u'w'}$, $\overline{u'^2}$, $\overline{v'^2}$, $\overline{w'^2}$; logarithmic velocity profile), the LRR Reynolds-stress equations reduce to a set of algebraic equations which determine the stresses. The choice $c_1 = 1.8$, $c_2 = 0.6$, $c_1' = 0.5$ yields $\sigma_u/u_* = 2.15$, $\sigma_v/u_* = 1.63$, $\sigma_w/u_* = 1.21$ in satisfactory agreement with measured values above the canopy in the experiments to be simulated. Then $k/u_*^2 = 4.37$ and the choice $C_3 = 1/4.37$ (for the constant in the expression for the 'cascade' conversion of SKE to WKE) ensures that at local equilibrium the dissipation rate matches the shear production rate $P = u_*^3/k_v z$.

3. Numerical Method

3.1. General approach

The general approach has been to follow the SIMPLE numerical method described by Patankar (1980). Although the ingenious and effective treatment of the mean pressure-mean velocity field coupling which is characteristic of SIMPLE is not needed for a

one-dimensional flow ($\overline{w} = 0$; $\partial\overline{p}/\partial x = 0$), other features of SIMPLE such as the scheme to ensure necessarily positive variables (e.g., TKE) remain positive recommend its use.

The equations are analytically integrated along the vertical axis between limits z_1 and z_2, e.g.,

$$[\overline{u'w'}]_{z_1}^{z_2} = -c_d a\overline{u}\,|\overline{u}|\,(z_2 - z_1)\,,$$

to obtain difference equations which express conservation in layers.

Odd velocity moments ($\overline{u}$, $\overline{u'^3}$, $\overline{u'w'^2}$, ...) are defined at grid points which are offset relative to the grid points for even moments ($\overline{u'w'}$, $\overline{u'^2}$, ...). This (staggered) grid is set up so that even-moment (Reynolds stress) grid points are at $z = H$ and at the top boundary. The lowest $\overline{u}$-grid point is at the ground. To each grid point there corresponds a 'control layer'. This choice of grid-point positioning is most natural because in the difference equation for each mth-order moment, differences of $(m + 1)$th-order moments arise.

The second-order closure scheme yields diffusion terms in the Reynolds stress equation. Because of these diffusion terms, the difference equations are in effect 'neighbour' equations, relating each grid point value to its over- and under-lying neighbours. With special neighbour relations chosen for the boundary values, one may then solve for the column of values of $\overline{u'^2}$ (etc.) using a tridiagonal matrix algorithm. From an initial (crude) guess of the solution, one proceeds iteratively towards a final solution.

In the case of canopy flow, it is advantageous to treat the velocity $\overline{u}$ as being related not only to its immediate over- and under-lying velocity neighbours $\overline{u}_N$, $\overline{u}_S$, but also to its momentum-flux neighbours, i.e., to form a 'stress-velocity' (sv) column whose elements are

$$\ldots\ldots, \overline{u}, \overline{u'w'}, \overline{u}, \overline{u'w'}, \overline{u}, \overline{u'w'}, \overline{u}, \ldots$$

From the budget equations one may now form neighbour relations of the form

$$a_C sv_C = a_{NN} sv_{NN} + a_N sv_N + a_S sv_S + a_{SS} sv_{SS} + bsv\,.$$

With the addition of special relations at the boundaries, one now has to invert a penta-diagonal matrix to obtain the latest guess for the stress-velocity field given the present estimates of the coefficients a_C, $a_{NN} \ldots a_{SS}$ and the 'source term' bsv.

The reason for choosing to link the Reynolds-stress and velocity so tightly is clear from the form of the $\overline{u}$-momentum equation (1) and the fact that this equation yields no direct information on the mean velocity above the canopy; the $\overline{u}$-momentum equation states that $\overline{u'w'}$ = const. above the canopy, and one may obtain the $\overline{u}$-field above the canopy by an upward integration of the gradient $\partial\overline{u}/\partial z$ which appears in the above-canopy stress-equation.

3.2. Boundary conditions

At the top boundary, the normalized Reynolds stress takes the value -1. At the lower boundary, as is conventional, a shallow equilibrium wall layer has been assumed, so that from the mean velocity $u_p = \bar{u}(2)$ at the first grid point above ground z_p, one may define

$$u_* = \frac{0.4\bar{u}(2)}{\ln(z_p/z_0)} \quad \text{and} \quad \overline{u'w'}(1) = -u_*^2 u_p/|u_p|\,,$$

where z_0 is a roughness length appropriate to the underlying surface (solutions are very insensitive to the choice of this roughness length).

At both the upper boundary and at the ground, the vertical derivative of the velocity variance has been set to zero. An upper boundary condition on the mean velocity is not required. Clearly it would have been possible to improve agreement with observations by, for example, imposing observed values of the normal stresses at the top boundary (or at the ground). The approach taken here has been to avoid depending on knowledge one would not expect to have in any future application of this type of model. However, it must be admitted that the use of an optimized drag coefficient is a very important exception to this convention; one would not, in any application, have the luxury of being able to determine c_d from the measured wind and stress profiles.

3.3. Grid choice

All reported simulations were carried out with the stress levels (i.e., even velocity moments) chosen to lie at

$$z/H = 0.1\ [0.1]\ 0.3\ [0.05]\ 1.1\ [0.1]\ 2.0\ [0.2]\ 3.2\ [0.3]\ 3.5\ [0.5]\ 6.0\,,$$

where the number enclosed thus [ ] denotes the intervals used in progressing from the limits on either side. Velocity grid points were placed at the ground and midway between stress grid points. Fine resolution was found to be particularly important near the top of the canopy where gradients are streep and change rapidly. Solutions given are not claimed to be grid independent but it is expected that changes with further grid refinement would be small.

3.4. Numerical stability

If q^o denotes the 'old' estimate of q and q^n the new, the customary 'relaxation' procedure is to define

$$q = \alpha q^o + (1 - \alpha)q^n$$

as the 'relaxed' new estimate (where $\alpha < 1$). This procedure, which does not affect the final solution but only the rate of progress toward it, was found to be necessary to ensure numerical stability.

3.5. Criterion for convergence

Numerical integrations were terminated when the largest changes in $\bar{u}$, $\overline{u'w'}$ relative to the prior guess did not exceed $0.005u_{*H}$. This required of the order of 3 min computation time using the *C* language on an IBM PC.

During most of the hundreds of numerical integrations performed during this work, the author watched the sequence of estimates and the progress of the residuals in solution of the equation. A strong impression was formed that convergence towards a solution which agrees well with observations is more rapid and regular than progress towards a bad solution. This can be a useful indication that one is 'flogging a dead horse'.

4. Data

One of the difficulties in evaluating canopy flow models is the scarcity of observations which are sufficiently complete. One would like a detailed description of the canopy (area density versus height) and measured profiles of $\bar{u}$, $\overline{u'w'}$, $\overline{u'^2}$, $\overline{v'^2}$, $\overline{w'^2}$ (at least) within and well above the canopy. Furthermore, since the turbulent intensity is very high within a canopy, one must treat some of the available data-sets as suspect, owing to the special care needed to perform anemometry when the flow exhibits a huge range of angles of attack relative to the anemometer.

Wilson *et al.* (1982) measured profiles of turbulence statistics within a mature corn canopy using specially-designed servo-controlled split-film heat-transfer anemometers. Their Table I shows that the instrument comparisons on 2 August, 1977 and 4 August, 1977 indicate excellent consistency. The area density profile had been sampled on 29 July, 1977, and on 2 August, 1977, 37 samples of plant height yielded heights of 2.01 m to the top leaf, 2.25 m to the top of the tassels. It was decided to use the

TABLE I

Turbulence observations within a corn canopy, Elora, Ontario, Canada, 2 and 4 August, 1977

z/H	$\overline{u'w'}/\overline{u'w'_H}$	$\bar{u}/\bar{u}_H$	$\bar{u}/u_{*H}$	σ_u/u_{*H}	σ_v/u_{*H}	σ_w/u_{*H}
0.87	0.78	0.62	1.85	1.60	1.29	1.11
	0.79	0.63	2.01	1.65	1.28	1.11
	0.96	0.66	2.12	1.70	1.34	1.09
	0.96	0.67	2.07	1.70	1.29	1.09
0.81	0.63	0.47	1.57	1.39	1.40	1.09
	0.64	0.50	1.59	1.34	1.28	1.04
0.75	0.31	0.31	0.99	1.11	0.97	0.86
0.62	0.113	0.180	0.52	0.69	0.82	0.71
	0.126	0.182	0.57	0.72	0.82	0.73
0.50	0.049	0.126	0.43	0.60	0.69	0.53
	0.076	0.135	0.47	0.64	0.70	0.55
	0.039	0.108	0.34	0.58	0.73	0.54
	0.044	0.104	0.34	0.57	0.71	0.55
0.44	0.053	0.077	0.24	0.50	0.54	0.41
	0.057	0.078	0.24	0.53	0.56	0.43
0.33	0.0094	0.047	0.14	0.45	0.49	0.29
	0.022	0.044	0.13	0.48	0.49	0.31

measurements of these two days rather than the complete data-set in order to avoid the complication of the change in canopy height which occurred over the entire period of the measurements. Table I presents the measured turbulence statistics for these two days. The upper anemometer height of 2.21 m has been defined to be the 'canopy height' (H = 2.21 m) since few tassles protruded above his level and one therefore expects little momentum flux divergence above this level.

Averaging together all data obtained with both anemometers at z = 2.21 m (7 half-hour comparisons), the canopy-top statistics were found to be:

$$\bar{u}/u_{*H} = 3.04\ (0.10)\,, \qquad \sigma_u/u_{*H} = 2.06\ (0.08)\,,$$

$$\sigma_v/u_{*H} = 1.65\ (0.09)\,, \qquad \sigma_w/u_{*H} = 1.13\ (0.02)\,,$$

where the sample standard deviation is given in brackets. Table II gives the single-sided leaf area density measured in 7 layers, each 0.33 m in depth. The LAI obtained by summation is 2.9.

TABLE II

Leaf area density profile corresponding to measurements of Table I

Layer (m)	$a(z)$ (m^{-1})
2.00–2.33	0.16
1.67–2.00	2.22
1.33–1.67	2.11
1.00–1.33	1.66
0.67–1.00	1.53
0.33–0.67	0.71
0.00–0.33	0.42

By integrating the momentum equation (1) from z = 0 to $z = H$ using the measured profiles of $\bar{u}$, $\overline{u'w'}$ and $a(z)$ and assuming a constant drag coefficient and that $\overline{u'w'}(0) = 0$, it was deduced that $c_d = 0.30$. Figure 2 shows the profile of $\overline{u'w'}$ obtained by integrating Equation (1) using $c_d = 0.30$, and the observed $\bar{u}(z)$, $a(z)$. The agreement with the observations is not very good. Bearing in mind the sampling problem inherent in the determination of $a(z)$, one should accept the likelihood that there will always be a degree of error in the conformity of observations with Equation (1). For present purposes, it was decided to eliminate this problem by using the measured $\bar{u}(z)$, $\overline{u'w'}(z)$ to deduce

$$c_d a = -(\partial\overline{u'w'}/\partial z)/\bar{u}^2\,.$$

This value of $c_d a$ was then used in the numerical model, so that the measured profile of $a(z)$ was not needed.

Model simulations have also been performed for the wind-tunnel canopy flow described by Raupach *et al.* (1986). The 'tombstone canopy' was an array of vertical

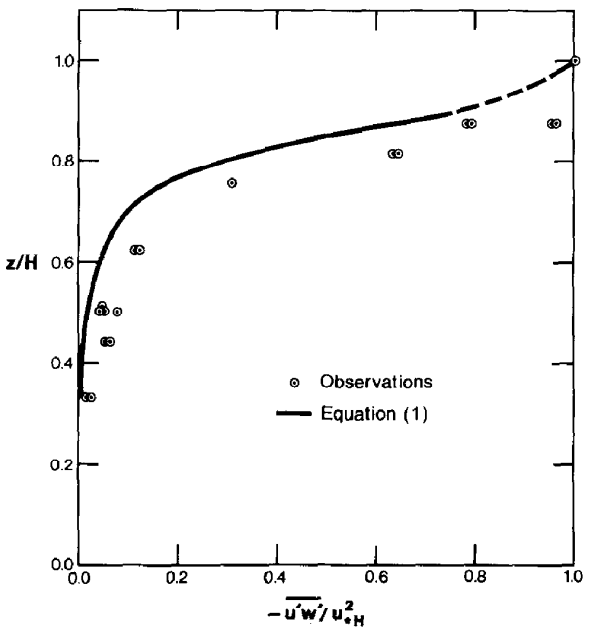

Fig. 2. Comparison of observed profile of $\overline{u'w'}$ within a corn canopy with the profile obtained by integrating the momentum equation (1) with a constant drag coefficient and the observed profiles of leaf area density and mean velocity $\bar{u}(z)$.

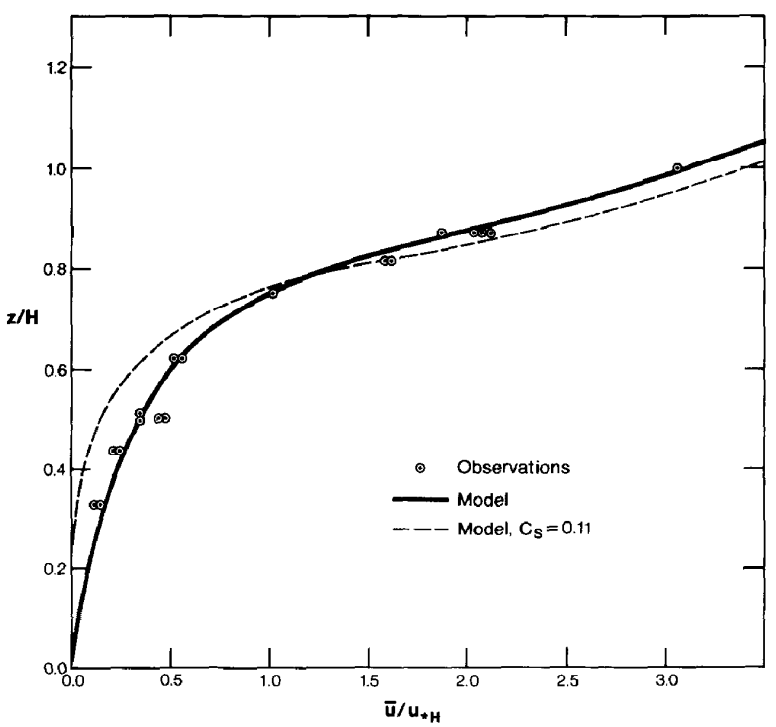

Fig. 3. Comparison of model prediction and observed mean wind profile within the corn canopy.

bars arranged in a regular diamond pattern. In the measurement section, the flow was in approximate streamwise equilibrium, and velocity statistics were measured using a specially-developed three-wire probe. The profiles which have been used here were evaluated from the measurements at $x \cong 1.5$ m. Specifically, the wind profile is the spatial average $\langle \overline{u} \rangle$ measured with a sonic anemometer at $x = 1.25$ m (their Figure 3(c)), while u'^2 was obtained from the given profile at a central position in the diamond cell at $x = 1.5$ m.

The canopy frontal area index was 0.23 which, given the canopy height $H = 0.06$ m, implies that the frontal area per unit volume was $a = 3.83\ \mathrm{m}^{-1}$.

Assuming $(\overline{u'w'})_0 = 0$ and applying the measured wind profile within the momentum equation (1), the author found that a value $c_d = 1.15$ is necessary to predict $(\overline{u'w'})_H$ correctly. This is higher than the value of 0.8 quoted by Raupach *et al.* obtained by the same process; the reason for this difference is unknown. In simulations here, $c_d = 1.15$ and $aH = 0.23$ (simulations with $c_d = 0.8$ were distinctly inferior).

Because the tombstone canopy flow is not strictly one-dimensional (see, for example, the momentum flux gradient above the canopy), simulations were performed with the top grid point at $z/H = 2$.

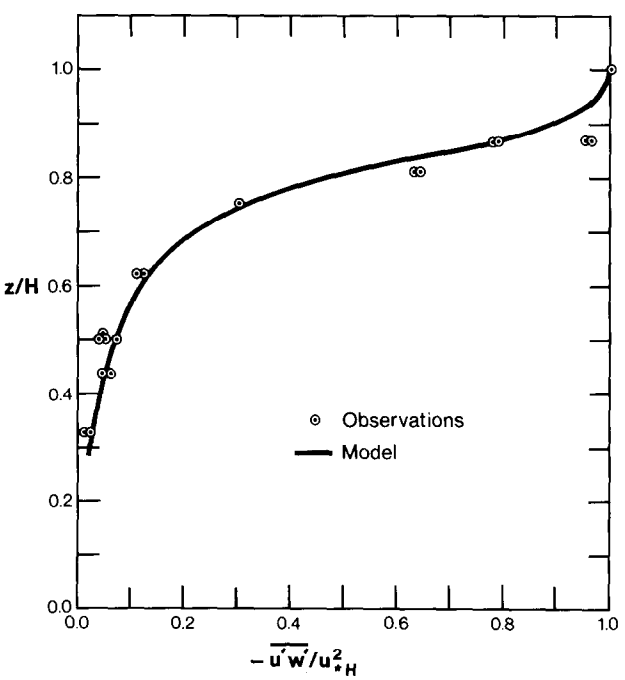

Fig. 4. Comparison of modelled and observed profiles of the shear stress $\overline{u'w'}$ within the corn canopy.

5. Results

5.1. Corn canopy

Figure 3 compares the prediction of the numerical model with the Elora observations within a corn canopy. Unfortunately, above canopy measurements were not carried out; according to the simulation, the wind profile becomes logarithmic with respect to z a very short distance above the canopy ($z/H \geq 1.4$) with slope $\partial(\bar{u}/u_*)/\partial \ln z = 1/k_v$ and with effective roughness length $z_0 \cong 0.18H$. This is a consequence of the fact that the length scale used in the parameterization of viscous dissipation (which in turn affects the effective eddy viscosity above the canopy) was z rather than $z - d$ (where d is a displacement height). With hindsight, a displacement length should have been included. In any case, the within-canopy profile is predicted accurately. The dashed line in Figure 3 shows the prediction with $c_s = C_{s0}$, which is certainly inferior. Figure 4 shows that the predicted profile of momentum flux is in good agreement with observation; this need hardly be stated – an accurate wind profile in conjunction with the 'correct' $c_d a$ yields an accurate momentum flux profile automatically (i.e., the two are linked).

Figures 5 and 6 compare observed and predicted profiles of σ_u/u_{*H} and σ_w/u_{*H}. The modification of c_s has a very large effect on the velocity fluctuation variances deep in

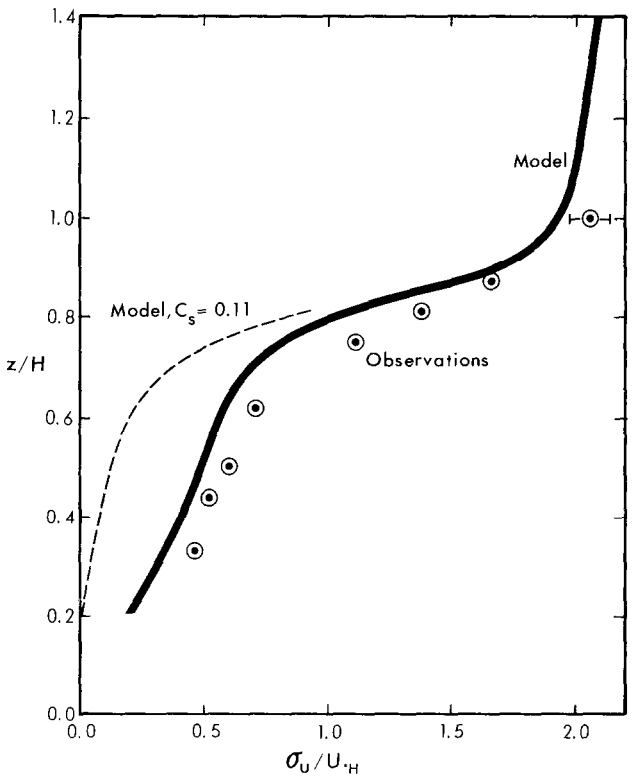

Fig. 5. Comparison of modelled and observed profiles of the standard deviation of the streamwise velocity fluctuation σ_u within and above the corn canopy.

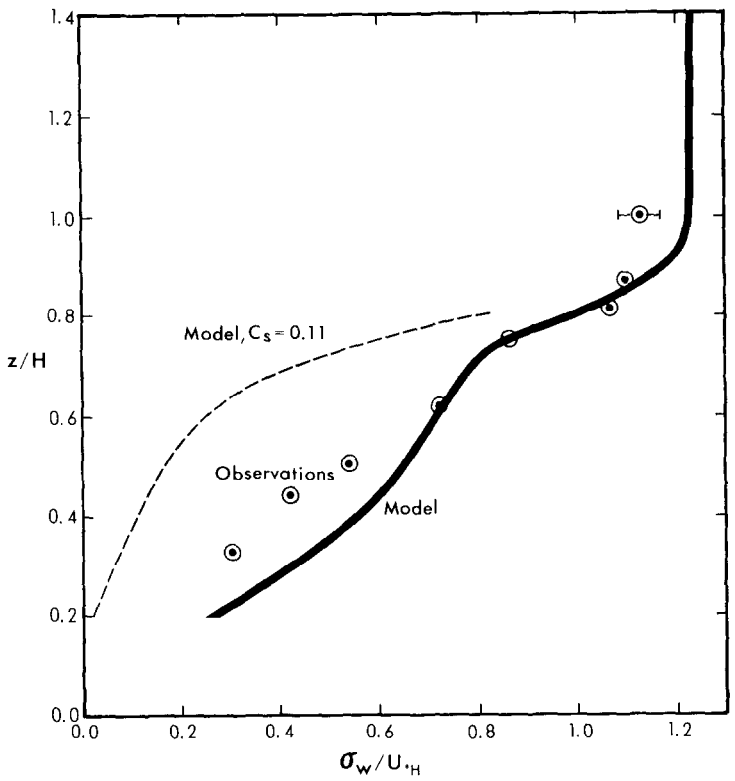

Fig. 6. Comparison of modelled and observed profiles of the standard deviation of the vertical velocity σ_w within and above the corn canopy.

the canopy, in contrast to its modest effect on the wind and momentum-flux profiles. Noting that there is no empirical source/sink term included in the $\overline{u'w'}$ equation and the weak foundation for the chosen empirical variance-sinks (especially deep in the canopy), one wonders if the need for a modification in c_s to yield more transport of variance into the lower canopy has arisen because the destruction rate has been overestimated; alternatively, the parameterisation of turbulent transport may be fundamentally inadequate.

The computed components of the SKE budget equation are in qualitative agreement with estimates derived from observations by Shaw and Seginer (1985). Viscous dissipation of SKE was calculated to be of negligible importance within the canopy. The most notable difference is that according to these calculations the region $z \approx H$ (actually, $0.95 \leqq z/H \leqq 1.2$) is an exporter of SKE (by turbulent transport) to other regions, owing to an excess of shear production ($|\overline{u'w'}|$ still large, $\partial\bar{u}/\partial z$ very large, but small area density at large z/H so that form drag is not yet dominant). This contrasts with the indication of Shaw and Seginer, which suggests that at $z \approx H$, SKE is imported (gained) by turbulent transport (as at lower levels). However, Shaw and Seginer have interpolated between measurements at $z/H \sim 0.9$ and $z/H \sim 1.3$ and may thereby have missed a

reversal in the sign of turbulent transport just below $z = H$. It is worth noting that predictions of Wilson and Shaw (1977) and observations of Raupach *et al.* (1986) indicate the region near $z = H$ to be an exporter of *total* TKE.

5.2. Tombstone canopy

Figure 7 shows that the numerical model yields a good prediction of the measured horizontal-average wind profile (and, though not shown, a correspondingly good prediction of the momentum flux). Raupach *et al.* observed quite large spatial variations in the single-point mean velocity within measured cells. The simulations were initially

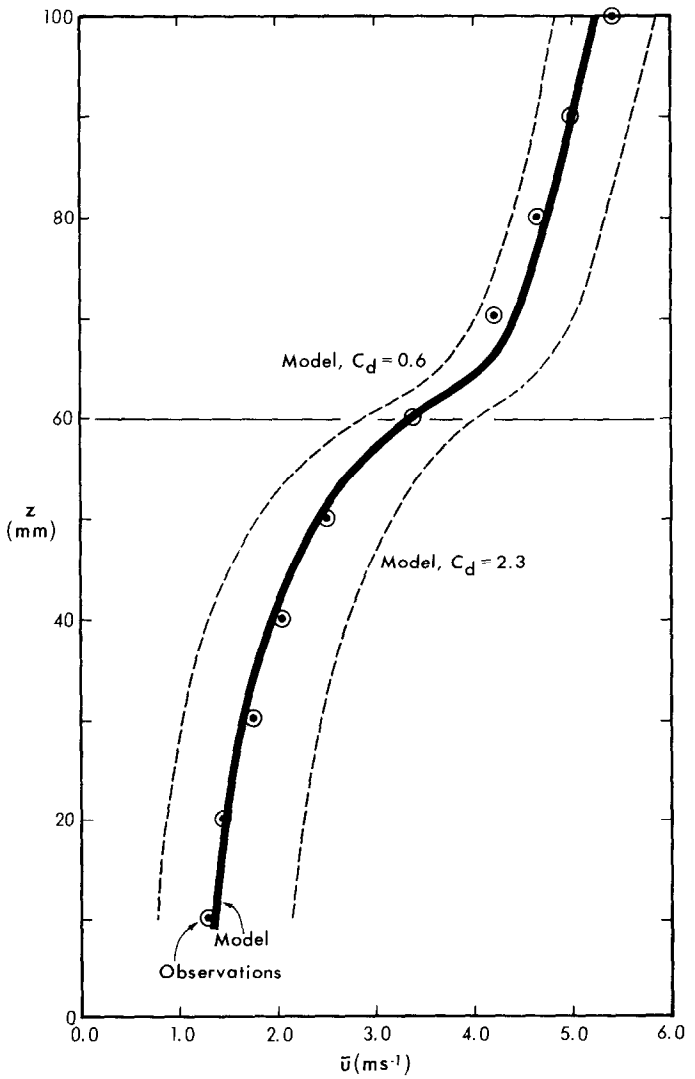

Fig. 7. Comparison of modelled and observed wind profile $\bar{u}(z)$ within and above the wind tunnel canopy. The dashed curves give the prediction with increased and decreased values for the drag coefficient.

compared with the single-point profile at cell centre at $x = 2.5$ m; the agreement was less pleasing. It is of interest (though uncertain significance) that the numerical profile is much closer to the spatially averaged wind profile than the single-point profile.

Also shown on Figure 7 are the profiles generated with $c_d = (0.5, 2.0) \times 1.15$. These are included to give some idea of the consequences of an imprecise knowledge of the true drag coefficient (which in most applications would be unknown).

Figure 8 shows the predicted and observed profiles of σ_u for the tombstone canopy. The modification of c_s has almost no impact on the simulation of the tombstone canopy, since the frontal area index of 0.23 is quite small (relative to the LAI 2.9 of the corn canopy). The rather poor model prediction for σ_u deep in the canopy is reminiscent of the poor predictions for the corn canopy when the modification to c_s is not used (Figure 5). This probably means that the parameterisation of turbulent transport used here is inadequate.

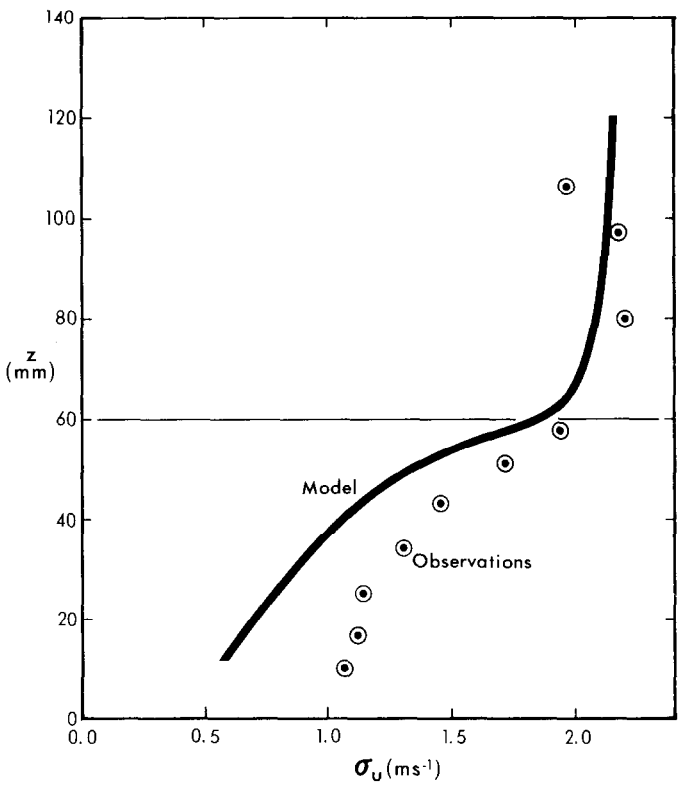

Fig. 8. Comparison of modelled and observed profiles of the standard deviation of the streamwise velocity fluctuation σ_u within and above the wind tunnel canopy.

6. Discussion

In evaluating the usefulness of this or any other canopy flow model, one must give some thought to the level of accuracy which it is meaningful and realistic to strive for. In at least some canopies there are large variations in mean windspeed in the horizontal plane (due to sheltering by individual plants). Baldocchi *et al.* (1983) measured differences of the order of 50% between windspeeds within and between rows of a soybean canopy. The spatial variations in the tombstone canopy have already been mentioned; these amounted to of the order of 25% variation.

It therefore seems likely that models which yield only a single estimate of windspeed for a given height (whether or not this single estimate is a point value or a horizontal average) will be of no use in any application which requires that windspeed be estimated to an accuracy of better than about 25%.

One of the most likely applications of a canopy flow model is as a component of a canopy evapotranspiration and/or crop growth model (see, for example, Hwang and Shaw (1985) who used a second-order closure model, including vapor and heat transport, to examine the effectiveness of practices which aim to conserve water by reducing soil evaporation). In this context, the impact of the wind and turbulence estimates is primarily (or most strongly) upon the leaf boundary-layer resistances. Experimental evidence (Pearman *et al.*, 1972) is that leaf boundary-layer resistance scales with $\sqrt{V}$, where V is the instantaneous wind speed, so that percentage errors in transfer resistances are half the percentage errors in the wind estimates. Furthermore, even if $\sqrt{V}$ was predicted perfectly (or measured), actual values of the transfer coefficient may differ by as much as $\pm 50\%$ relative to the estimate obtained from the correlation employed. That is to say, even perfect wind estimates would lead to imperfect transfer coefficient estimates. In the cases of vapor transport from a dry canopy or CO_2 uptake, this gloomy situation is brightened somewhat by the fact that the leaf boundary-layer resistances will usually be much smaller than the stomatal resistance.

In view of the above comments, one might say that if we can predict the windspeed and turbulence to within $\pm 50\%$, we are doing as well as is realistic (from the point of view of within-canopy variations) and useful for the type of applications envisaged. In that case, the present generation of canopy flow models (and in fact much cruder models) should suffice for practical purposes, and if they do not, it is unlikely that future models will.

Note that it has here been pre-supposed that the drag coefficient c_d is independent of windspeed; within this framework, it is a foregone conclusion that one will predict, for given $a(z)$, a 'universal' profile of $\overline{u}/u_{*H}$ or $\overline{u}/\overline{u}_H$, having no sensitivity to the actual windspeed. The Elora observations support this framework (unique profile of $\overline{u}/\overline{u}_H$, or equivalently $u_{*H}^2 \propto u_H^2$), but other experiments have yielded neutral wind-profiles which are not invariant and do depend on absolute windspeed. The simplest interpretation of this is probably to allow the drag coefficient to depend upon the Reynolds number $\overline{u}d/\nu$, where $\overline{u}$ is the local windspeed and d the leaf characteristic dimension (see Raupach and

Thom, 1981). One would then have to introduce a further non-dimensional controlling input, say $\bar{u}_H/u_{*H}$, or, more conveniently, $\bar{u}_{\mathrm{TOP}}/u_*$ (i.e., conditions on both $\bar{u}$ and u_* at the top boundary).

While on the topic of the drag coefficient, it is worth noting that, to date, canopy flow models have achieved good agreement with observation partly because the drag coefficient has been available as a freely assignable constant or has been deduced directly from the measured wind, stress, and area density profiles. This is unsatisfactory since in any application, it will be necessary to provide an independent estimate of the drag coefficient. This is not an easy task, even given the drag coefficient for a plant part in a uniform flow, due to the mutual interaction of the plant elements which reduces the effective drag coefficient.

7. Conclusion

This second-order closure scheme yields reasonably good predictions of the wind statistics in two rather different canopies. However, it is not claimed that this closure scheme has general validity, and a search for physically-sound closure approximations for canopy flow must be encouraged.

The main distinction between this and earlier models is that a dual frequency band turbulent kinetic energy balance has been employed, and the ratio k/ε of the low-frequency band TKE to its dissipation rate has served as the required turbulence time-scale. While this partly removes the need to arbitrarily specify a turbulence length scale (a length scale is still imposed for the viscous dissipation term), it must be admitted that there is a counterbalancing empiricism involved in formulating the two-band model. Nevertheless, it does seem worthwhile to aim to model the additional turbulent kinetic energy transformation pathways which occur in canopy flow because their importance, at least in dense canopies, has been clearly demonstrated.

References

Baldocchi, D. D., Verma, S. B., and Rosenburg, N. J.: 1983, 'Characteristics of Air Flow Above and Within Soybean Canopies', *Boundary-Layer Meteorol.* **25**, 43–54.

Deardorff, J. W.: 1978, 'Closure of Second- and Third-Moment Rate Equations for Diffusion in Homogeneous Turbulence', *Phys. Fluids* **21**, 525–530.

Finnigan, J. J.: 1979, 'Turbulence in Waving Wheat. II. Structure of Momentum Transfer', *Boundary-Layer Meteorol.* **16**, 213–236.

Finnigan, J. J.: 1985, 'Turbulent Transport in Flexible Plant Canopies', in B. A. Hutchison and B. B. Hicks (eds.), The Forest-Atmosphere Interaction, D. Reidel Publ. Co., Dordrecht, Holland.

Gibson, M. M. and Launder, B. E.: 1978, 'Ground Effects on Pressure Fluctuations in the Atmospheric Boundary Layer', *J. Fluid Mech.* **86**, 491–511.

Hanjalic, K. and Launder, B. E.: 1972, 'A Reynolds Stress Model of Turbulence and its Application to Thin Shear Flows', *J. Fluid Mech.* **52**, 609–638.

Hanjalic, K., Launder, B. E., and Schiestel, R.: 1980, 'Multiple Time-Scale Concepts in Turbulent Transport Modelling', in L. J. S. Bradbury, F. Durst, B. E. Launder, F. W. Schmidt, and J. H. Whitelaw (eds.), *Turbulent Shear Flows 2*, Springer-Verlag, Berlin.

Hwang, C. and Shaw, R. H.: 1985, 'Evaluation of the Relationship between Transpiration and Soil Evaporation', pp. 33–36 of the preprint volume, 17th Conference of the American Meteorol. Soc. on Agricultural and Forest Meteorology, Scottsdale, Arizona, May 1985.

Launder, B. E., Reece, G. J., and Rodi, W.: 1975, 'Progress in the Development of a Reynolds-Stress Turbulence Closure', *J. Fluid Mech.* **68**, 537–566.

Leonard, A.: 1985, 'Computing Three-Dimensional Incompressible Flows with Vortex Elements', *Ann. Rev. Fluid Mech.* **17**, 523–559.

Li, Z. J., Miller, D. R., and Lin, J. D.: 1985: 'A First-Order Closure Scheme to Describe Counter-Gradient Momentum Transport in Plant Canopies', *Boundary-Layer Meteorol.* **33**, 77–83.

McAneney, K. J. and Judd, M. J.: 1987, 'Comparative Shelter Strategies for Kiwifruit: A Mechanistic Interpretation of Wind Damage Measurements', *Agric. Forest Meteorol.* **39**, 225–240.

Meyers, T. and Paw U, K. T.: 1986, 'Testing of a Higher Order Closure Model for Modelling Airflow Within and Above Plant Canopies', *Boundary-Layer Meteorol.* **37**, 297–311.

Mulhearn, P. J.: 1978, 'Turbulent Flow Over a Periodic Rough Surface', *Phys. Fluids* **21**, 1113–1115.

Mulhearn, P. J. and Finnigan, J. J.: 1978, 'Turbulent Flow Over a Very Rough, Random Surface', *Boundary-Layer Meteorol.* **15**, 109–132.

Patankar, S. V.: 1980, 'Numerical Heat Transfer and Fluid Flow', *Series in Computational Methods in Mechanics and Thermal Science*, Hemisphere Publ. Co., London.

Pearman, G. I., Weaver, H. L., and Tanner, C. B.: 1972, 'Boundary Layer Heat Transfer Coefficients Under Field Conditions', *Agricultural Meteorol.* **10**, 83–92.

Raupach, M. R.: 1987, 'A Lagrangian Analysis of Scalar Transfer in Vegetation Canopies', *Quart. J. Roy. Meteorol. Soc.* **113**, 107–120.

Raupach, M. R. and Shaw, R. H.: 1982, 'Averaging Procedures for Flow Within Vegetation Canopies', *Boundary-Layer Meteorol.* **22**, 79–90.

Raupach, M. R. and Thom, A. S.: 1981, 'Turbulence In and Above Plant Canopies', *Ann. Rev. Fluid Mech.* **13**, 97–129.

Raupach, M. R., Coppin, P. A., and Legg, B. J.: 1986, 'Experiments on Scalar Dispersion Within a Model Plant Canopy. Part I: The Turbulence Structure', *Boundary-Layer Meteorol.* **35**, 21–52.

Shaw, R. H.: 1985, 'Calculation of the Third Moments of the Velocity Field in a Canopy Layer', pp. 77–79 of the preprint volume, 17th Conference of the American Meteorological Society on Agricultural and Forest Meteorology, Scottsdale, Arizona, May 1985.

Shaw, R. H. and Seginer, I.: 1985: 'The Dissipation of Turbulence in Plant Canopies', pp. 200–203, preprint volume, 7th Symposium of the American Meteorological Society on Turbulence and Diffusion, Boulder, Colorado, November 1985.

Shaw, R. H., Tavangar, J., and Ward, D. P.: 1983, 'Structure of the Reynolds Stress in a Canopy Layer', *J. Clim. Appl. Meteorol.* **22**, 1922–1931.

Shir, C. C.: 1973, 'A Preliminary Numerical Study of Atmospheric Turbulent Flows in the Idealised Planetary Boundary Layer', *J. Atmos. Sci.* **30**, 1327–1339.

Taylor, G. I.: 1921, 'Diffusion by Continuous Movements', *Proc. London Math. Soc.*, Ser. 2, Vol. 20, 196–212.

Wilson, J. D.: 1985, 'Numerical Studies of Flow Through a Windbreak', *J. Wind Eng. and Ind. Aero.* **21**, 119–154.

Wilson, J. D., Ward, D. P., Thurtell, G. W., and Kidd, G. E.: 1982, 'Statistics of Atmospheric Turbulence Within and Above a Corn Canopy', *Boundary-Layer Meteorol.* **24**, 495–519.

Wilson, N. R. and Shaw, R. H.: 1977, 'A Higher Order Closure Model for Canopy Flow', *J. Appl. Meteorol.* **16**, 1197–1205.